



# Quantum walks in artificial electric and gravitational fields



Giuseppe Di Molfetta<sup>a</sup>, Marc Brachet<sup>b</sup>, Fabrice Debbasch<sup>a,\*</sup>

<sup>a</sup> LERMA, UMR 8112, UPMC and Observatoire de Paris, 61 Avenue de l'Observatoire 75014 Paris, France

<sup>b</sup> Laboratoire de Physique Statistique, Ecole Normale Supérieure, UPMC Université Paris 06, Université Paris Diderot, CNRS, 24 rue Lhomond, 75005 Paris, France

## HIGHLIGHTS

- The continuous limit of quantum walks on the line is investigated systematically through a new method.
- In all cases but one, the continuous limit coincides with the propagation of a Dirac fermion.
- Inhomogeneities in the walk transcribe as artificial electric and gravitational fields.
- New, state of the art simulations of a quantum walk propagating in an artificial electric field.
- New, state of the art simulations of a quantum walk propagating in and around an artificial black hole.

## ARTICLE INFO

### Article history:

Received 20 August 2013  
Received in revised form 19 November 2013  
Available online 9 December 2013

### Keywords:

Quantum walks  
Artificial gauge fields  
Low dimensional physics  
Quantum optics

## ABSTRACT

The continuous limit of quantum walks (QWs) on the line is revisited through a new, recently developed method. In all cases but one, the limit coincides with the dynamics of a Dirac fermion coupled to an artificial electric and/or relativistic gravitational field. All results are carefully discussed and illustrated by numerical simulations. Possible experimental realizations are also addressed.

© 2013 Elsevier B.V. All rights reserved.

## 1. Introduction

QWs are simple formal analogues of classical random walks. They were first considered by Feynman [1] as possible discretizations of the free Dirac dynamics in flat space–time. They have been introduced in the physics literature by Refs. [2,3] and the continuous-time version first appeared in Ref. [4]. They have been realized experimentally in Refs. [5–12] and are important in many fields, ranging from fundamental quantum physics [12,13] to quantum algorithmics [14,15], solid state physics [16–19] and biophysics [20,21]. Following Feynman's idea, several authors have studied the continuous limit of various QWs. The first publications [22–24,1,25–28] only addressed QWs with constant coefficients and recent work has extended the discussion to QWs with time- and space-dependent coefficients [29–32], in both (1+1) and (1+2) space–time dimensions. In particular, a new method was developed in Refs. [29–32] to investigate the continuous limit of QWs with nonconstant coefficients. This method delivers interesting results, not only for standard QWs, but also for 'derived' QWs obtained from original QWs by keeping only one time-step out of two [32]. So far, this new method has only been applied to particular families of walks. This article presents the systematic application of this method to all QWs in (1+1) space–time dimensions. The main conclusions are: (i) all families of walks do not admit a continuous limit (ii) when the limit exists, it

\* Corresponding author. Tel.: +33 144277286; fax: +33 144277287.  
E-mail address: [fabrice.debbasch@gmail.com](mailto:fabrice.debbasch@gmail.com) (F. Debbasch).

coincides, in all cases but one, with the dynamics of a Dirac fermion coupled to an artificial electric field and/or relativistic gravitational field. These theoretical conclusions are illustrated by numerical simulations. Connections with previous results as well as other topics like transport in graphene are discussed and possible experimental realizations are also mentioned.

## 2. Fundamentals

We consider quantum walks defined over discrete time and discrete one-dimensional space, driven by time- and space-dependent quantum coins acting on a two-dimensional Hilbert space  $\mathcal{H}$ . The walks are defined by the following finite difference equations, valid for all  $(j, m) \in \mathbb{N} \times \mathbb{Z}$ :

$$\begin{bmatrix} \psi_{j+1,m}^L \\ \psi_{j+1,m}^R \end{bmatrix} = B(\theta_{j,m}, \xi_{j,m}, \zeta_{j,m}, \alpha_{j,m}) \begin{bmatrix} \psi_{j,m+1}^L \\ \psi_{j,m-1}^R \end{bmatrix}, \tag{1}$$

where

$$B(\theta, \xi, \zeta, \alpha) = e^{i\alpha} \begin{bmatrix} e^{i\xi} \cos \theta & e^{i\zeta} \sin \theta \\ -e^{-i\zeta} \sin \theta & e^{-i\xi} \cos \theta \end{bmatrix}. \tag{2}$$

This operator is in  $U(2)$ , and is in  $SU(2)$  only for  $\alpha = p\pi$ ,  $p \in \mathbb{Z}$ , and  $\theta, \xi$  and  $\zeta$  are then called the three Euler angles of  $B$ . The index  $j$  labels instants and the index  $m$  labels spatial points. The two functions  $\psi^L$  and  $\psi^R$  can be interpreted as the components of a wave function  $\Psi$  on a certain orthonormal basis  $(b_L, b_R)$  independent of  $j$  and  $m$ . These two components code for the probability amplitudes of the particle jumping towards the left or towards the right. The total probability  $\pi_j = \sum_m (|\psi_{j,m}^L|^2 + |\psi_{j,m}^R|^2)$  is independent of  $j$ , that is, it is conserved by the walk. The set of angles  $\{\theta_{j,m}, \xi_{j,m}, \zeta_{j,m}, \alpha_{j,m}, (j, m) \in \mathbb{N} \times \mathbb{Z}\}$  defines the walks and is at this stage arbitrary.

Consider now, for all  $(n, j) \in \mathbb{N}^2$ , the collection  $W_j^n = (\Psi_{k,m})_{k=nj, m \in \mathbb{Z}}$ . This collection represents the state of the quantum walk at ‘time’  $k = nj$ . For any given  $n$ , the collection  $S^n = (W_j^n)_{j \in \mathbb{Z}}$  thus represents the entire history quantum walk observed through a stroboscope of ‘period’  $n$ . The evolution equations for  $S^n$  are those linking  $W_{j+1}^n$  to  $W_j^n$  for all  $j$ . These can be deduced from the original evolution Eqs. (1) and (2) of the walk, which also coincide with the evolution equations of  $S^1$ . For example, the evolution equations of  $S^2$  read

$$\begin{aligned} \psi_{j+2,m}^L &= A_{j,m}^L \psi_{j,m+2}^L + B_{j,m}^L \psi_{j,m}^L + C_{j,m}^L \psi_{j,m}^R + D_{j,m}^L \psi_{j,m-2}^R \\ \psi_{j+2,m}^R &= A_{j,m}^R \psi_{j,m+2}^R + B_{j,m}^R \psi_{j,m}^R + C_{j,m}^R \psi_{j,m}^L + D_{j,m}^R \psi_{j,m-2}^L \end{aligned} \tag{3}$$

where

$$\begin{aligned} A_{j,m}^L &= c_{j+1,m} c_{j,m+1} e^{i(\alpha_{j+1,m} + \xi_{j+1,m} + \alpha_{j,m+1} + \xi_{j,m+1})} \\ B_{j,m}^L &= -s_{j+1,m} s_{j,m-1} e^{i(\alpha_{j+1,m} + \zeta_{j+1,m} + \alpha_{j,m-1} - \zeta_{j,m-1})} \\ C_{j,m}^L &= c_{j+1,m} s_{j,m+1} e^{i(\alpha_{j+1,m} + \xi_{j+1,m} + \alpha_{j,m+1} + \zeta_{j,m+1})} \\ D_{j,m}^L &= s_{j+1,m} c_{j,m-1} e^{i(\alpha_{j+1,m} + \zeta_{j+1,m} + \alpha_{j,m-1} - \xi_{j,m-1})}, \end{aligned} \tag{4}$$

$$\begin{aligned} A_{j,m}^R &= -s_{j+1,m} c_{j,m+1} e^{i(\alpha_{j+1,m} - \zeta_{j+1,m} + \alpha_{j,m+1} + \xi_{j,m+1})} \\ B_{j,m}^R &= -s_{j,m-1} c_{j+1,m} e^{i(\alpha_{j+1,m} - \xi_{j+1,m} + \alpha_{j,m-1} - \zeta_{j,m-1})} \\ C_{j,m}^R &= -s_{j+1,m} s_{j,m+1} e^{i(\alpha_{j+1,m} - \zeta_{j+1,m} + \alpha_{j,m+1} + \zeta_{j,m+1})} \\ D_{j,m}^R &= c_{j,m-1} c_{j+1,m} e^{i(\alpha_{j+1,m} - \xi_{j+1,m} + \alpha_{j,m-1} - \xi_{j,m-1})}, \end{aligned} \tag{5}$$

with  $c_{jm} = \cos(\theta_{j,m})$  and  $s_{jm} = \sin(\theta_{j,m})$ .

The QWs defined by (1) admit a remarkable exact  $U(1)$  gauge invariance. Consider indeed an arbitrary set of numbers  $\{\phi_{jm}, (j, m) \in \mathbb{N} \times \mathbb{Z}\}$ , and write  $\Psi_{jm} = \Psi'_{jm} \exp(i\phi_{jm})$ . A straightforward computation shows that  $\Psi'$  obeys

$$\begin{bmatrix} \psi'_{j+1,m}{}^L \\ \psi'_{j+1,m}{}^R \end{bmatrix} = B(\theta'_{j,m}, \xi'_{j,m}, \zeta'_{j,m}, \alpha'_{j,m}) \begin{bmatrix} \psi'_{j,m+1}{}^L \\ \psi'_{j,m-1}{}^R \end{bmatrix}, \tag{6}$$

with

$$\begin{aligned} \alpha'_{j,m} &= \alpha_{j,m} + \frac{\sigma_{j,m}}{2} \\ \xi'_{j,m} &= \xi_{j,m} + \delta_{j,m} \\ \zeta'_{j,m} &= \zeta_{j,m} - \delta_{j,m} \\ \theta'_{j,m} &= \theta_{j,m} \end{aligned} \tag{7}$$

and

$$\sigma_{j,m} = \phi_{j,m+1} + \phi_{j,m-1} - 2\phi_{j+1,m} \quad (8)$$

$$\delta_{j,m} = \frac{\phi_{j,m+1} - \phi_{j,m-1}}{2}. \quad (9)$$

It can also be shown that the  $S^2$ -type QWs admit the same discrete invariance. As detailed in Sections 4 and 5, this discrete gauge invariance transcribes in the continuous limit into the standard continuous  $U(1)$  gauge invariance of Maxwell electromagnetism.

To investigate the continuous limit of a collection  $S^n$ , we first introduce a time step  $\Delta t$  and a space step  $\Delta x$ . We then consider that  $\Psi_{jm}, \theta_{jm}, \xi_{jm}, \zeta_{jm}$  and  $\alpha_{jm}$  are the values taken by a two-component wave function  $\Psi$  and by four functions  $\theta, \xi, \zeta$  and  $\alpha$  at the space–time point  $(t_j = j\Delta t, x_m = m\Delta x)$ . Thus, Eq. (1) transcribes into

$$\begin{bmatrix} \psi^L(t_j + \Delta t, x_m) \\ \psi^R(t_j + \Delta t, x_m) \end{bmatrix} = B(\theta(t_j, x_m), \xi(t_j, x_m), \zeta(t_j, x_m), \alpha(t_j, x_m)) \begin{bmatrix} \psi^L(t_j, x_m + \Delta x) \\ \psi^R(t_j, x_m - \Delta x) \end{bmatrix}. \quad (10)$$

We finally suppose that  $\Psi$  and  $\theta$  are at least twice differentiable with respect to both space and time variables for all sufficiently small values of  $\Delta t$  and  $\Delta x$ . The formal continuous limit of  $S^n$  is defined as the couple of partial differential equations (PDEs) obtained from the discrete-time evolution equations defining  $S^n$  by letting both  $\Delta t$  and  $\Delta x$  tend to zero.

### 3. How to determine the continuous limit

Let us introduce a time scale  $\mathcal{T}$ , a length-scale  $\mathcal{L}$ , an infinitesimal  $\epsilon$  and write

$$\begin{aligned} \Delta t &= \epsilon \mathcal{T} \\ \Delta x &= \epsilon^\delta \mathcal{L}, \end{aligned} \quad (11)$$

where  $\delta > 0$  allows  $\Delta t$  and  $\Delta x$  to tend to zero differently. We also allow the angles defining the walk to depend on  $\epsilon$  and characterize the  $\epsilon$ -dependence of these angles near  $\epsilon = 0$  by the following scaling laws:

$$\begin{aligned} \theta_\epsilon(t, x) &= \theta_0(t, x) + \bar{\theta}(t, x)\epsilon^\omega \\ \xi_\epsilon(t, x) &= \xi_0(t, x) + \bar{\xi}(t, x)\epsilon^\beta \\ \zeta_\epsilon(t, x) &= \zeta_0(t, x) + \bar{\zeta}(t, x)\epsilon^\gamma \\ \alpha_\epsilon(t, x) &= \alpha_0(t, x) + \bar{\alpha}(t, x)\epsilon^\eta, \end{aligned} \quad (12)$$

where the four exponents  $\omega, \beta, \gamma$  and  $\eta$  are all positive. We also suppose that all functions are at least  $C^2$  in  $t$  and  $x$ . The above relations define 1-jets of quantum walks. We finally denote by  $\mathcal{B}_\epsilon(t, x)$  the matrix  $B(\theta_\epsilon(t, x), \xi_\epsilon(t, x), \zeta_\epsilon(t, x), \alpha_\epsilon(t, x))$ .

Expand now the original discrete equations obeyed by a jet  $S_\epsilon^n$  around  $\epsilon = 0$ . A necessary and sufficient condition for the expansion to be self-consistent at order 0 in  $\epsilon$  is that  $\mathcal{B}_0^n(t, x) = 1$  for all  $t$  and  $x$  (note from Eq. (1) that this condition is self-evident for  $n = 1$ ). This transcribes into a constraint for the zeroth-order angles  $\theta_0, \xi_0, \zeta_0, \alpha_0$ .

Suppose this constraint is satisfied. The differential equations defining the continuous limit are obtained from the expansion by stating that the next lowest order contribution in  $\epsilon$  identically vanishes. If one excepts zeroth-order terms, the terms of lowest order in the expansion scale as  $\epsilon, \epsilon^\delta, \epsilon^\omega, \epsilon^\beta, \epsilon^\gamma, \epsilon^\eta$  (see for example the similar expansions performed on particular simple quantum walks and presented in Refs. [30,31]). The richest and most interesting scaling is thus  $\delta = \omega = \beta = \gamma = \eta = 1$ , because this makes all the above terms of the same order and, thus, delivers a differential equation with a maximum number of contributions. This scaling will be retained in the remainder of this article.

Note that Eqs. (11) and (12) have actually very different meanings. Indeed, (11) states that the relative variations of  $\Psi$  between  $j + 1, m$  and  $j, m \pm 1$  should be small, while (12) states that the angles defining the walk do not deviate much from their zeroth-order values.

We will now present in detail the continuous limit of the jets  $S_\epsilon^n$  for both  $n = 1$  and  $n = 2$ .

## 4. Limit of $S_\epsilon^1$

### 4.1. Zeroth-order values of the angles

The constraint on the zeroth-order angles reads

$$\begin{aligned} \sin \theta_0 &= 0 \\ e^{i(\alpha_0 + \xi_0)} \cos \theta_0 &= 1 \\ e^{i(\alpha_0 - \xi_0)} \cos \theta_0 &= 1. \end{aligned} \quad (13)$$

The above relations imply  $\theta_0 = k\pi, \alpha_0 = (k + k_+ + k_-)\pi, \xi_0 = (k_+ - k_-)\pi, (k, k_+, k_-) \in \mathbb{Z}^3$ . The angle  $\zeta_0$  does not enter this constraint and is therefore an arbitrary function of  $t$  and  $x$ . For a given value of  $\epsilon$ , there is thus no meaningful distinction between  $\zeta_0$  and  $\zeta$ . We will therefore from here on denote  $\zeta_0$  by  $\zeta$  in all equations, if only to simplify the notation.

### 4.2. Equations of motion

Let now  $T = t/\mathcal{T}$ ,  $X = x/\mathcal{L}$ ,  $x^\pm = (T \pm X)/2$  and  $\partial_\pm = \partial_{x^\pm} = \partial_T \pm \partial_X$ . The variables  $x^\pm$  are null coordinates in the flat 2D space–time. With these notations, the equations of motion for the continuous limit of  $S_\epsilon^1$  read

$$\begin{aligned} \partial_- \psi^L - i(\bar{\alpha} + \bar{\xi})\psi^L &= +\bar{\theta}e^{i(\theta_0 + \alpha_0 + \zeta)}\psi^R \\ \partial_+ \psi^R - i(\bar{\alpha} - \bar{\xi})\psi^R &= -\bar{\theta}e^{i(\theta_0 + \alpha_0 - \zeta)}\psi^L, \end{aligned} \tag{14}$$

where  $\theta_0$  and  $\alpha_0$  are arbitrary multiples of  $\pi$  (see the constraint above) and  $\zeta$  is an arbitrary real function of  $T$  and  $X$ .

Taken together, these two coupled first-order PDEs form a Dirac equation in  $(1 + 1)$  dimensions. Let us recall that, in flat two-dimensional space–times, the Clifford algebra can be represented by  $2 \times 2$  matrices acting on two-component spinors. This algebra admits two independent generators  $\gamma^0$  and  $\gamma^1$ , which can be represented by  $2 \times 2$  matrices obeying the usual anti-commutation relation

$$\{\gamma^a, \gamma^b\} = 2\eta^{ab}\mathcal{I}, \tag{15}$$

where  $\eta$  is the Minkowski metric and  $\mathcal{I}$  is the identity (unit) matrix. Consider the representation  $\gamma^0 = \sigma_1$  and  $\gamma^1 = -\sigma_1\sigma_3 = i\sigma_2$ , where  $\sigma_1, \sigma_2$  and  $\sigma_3$  are the three Pauli matrices:

$$\sigma_1 = \begin{bmatrix} 0 & 1 \\ 1 & 0 \end{bmatrix}, \quad \sigma_2 = \begin{bmatrix} 0 & -i \\ i & 0 \end{bmatrix}, \quad \sigma_3 = \begin{bmatrix} 1 & 0 \\ 0 & -1 \end{bmatrix}. \tag{16}$$

Eq. (14) can be recast in the following compact form:

$$(i\gamma^0 D_0 + i\gamma^1 D_1 - \mathcal{M})\Psi = 0, \tag{17}$$

where  $D_\mu = \partial_\mu - iA_\mu$ ,  $\partial_0 = \partial_T$ ,  $\partial_1 = \partial_X$ ,  $A_0 = \bar{\alpha}$ ,  $A_1 = -\bar{\xi}$ ,  $\mathcal{M} = \text{diag}(m^-, m^+)$  and  $m^\mp = \pm i\bar{\theta} \exp\{i(\theta_0 + \alpha_0 \pm \zeta)\}$ .

This equation describes the propagation in flat space–time of a Dirac spinor coupled to the Maxwell potential  $A$  (the corresponding electric field is  $E_X = \partial_T \bar{\xi} - \partial_X \bar{\alpha}$ ). The discrete gauge invariance presented in Section 2 degenerates accordingly into the standard local  $U(1)$  invariance associated with electromagnetism. Indeed, suppose that the numbers  $\phi_{jm}$  (see Section 2) are the values taken by a function  $\phi$  at space–time points ( $t_j = j\Delta t$ ,  $x_m = m\Delta x$ ). Expanding Eqs. (7) and (9) at first order in  $\epsilon$  delivers

$$\begin{aligned} \alpha' &= \alpha - \epsilon \frac{\partial \phi}{\partial T} \\ \xi' &= \xi + \epsilon \frac{\partial \phi}{\partial X} \\ \zeta' &= \zeta - \epsilon \frac{\partial \phi}{\partial X} \\ \theta' &= \theta. \end{aligned} \tag{18}$$

The first two equations imply

$$\begin{aligned} A'_0 &= \frac{1}{\epsilon} (\alpha' - \alpha_0) = \frac{1}{\epsilon} \left( \alpha - \epsilon \frac{\partial \phi}{\partial T} - \alpha_0 \right) = A_0 - \frac{\partial \phi}{\partial T} \\ A'_1 &= \frac{1}{\epsilon} (\xi_0 - \xi') = \frac{1}{\epsilon} \left( \xi_0 - \epsilon \frac{\partial \phi}{\partial X} - \xi \right) = A_X - \frac{\partial \phi}{\partial X}, \end{aligned} \tag{19}$$

which are simply the standard gauge transformation for the potential  $A$ . The fourth relation implies that the mass tensor  $\mathcal{M}$  is gauge invariant. Since the continuous limit equation of motion (14) depends only on  $\zeta_0$  (as opposed to  $\zeta$ ), the third equation is not relevant to the continuous limit investigated in this section.

The angles  $\theta_0$  and  $\alpha_0$  are both multiples of  $\pi$ . Both masses are therefore complex conjugates of each other. They are real, and therefore identical, if  $\zeta_0$  is an uneven multiple of  $\pi/2$ . They are both real and positive, equal to  $|\bar{\theta}|$ , if  $\zeta_0 = \theta_0 + \alpha_0 + \bar{\sigma} + (2p + 1)\pi/2$ , where  $\exp(i\bar{\sigma}) = \text{sgn } \bar{\theta}$  is the sign of  $\bar{\theta}$  and  $p$  is an arbitrary integer. Note that, even in this case, the mass may depend on both  $T$  and  $X$ .

## 5. Limit of $S_\epsilon^2$

### 5.1. Zeroth-order values of the angles

The constraint on the zeroth-order angles now reads

$$\begin{aligned} \cos \xi_0 \sin(2\theta_0) &= 0 \\ e^{2i\alpha_0} (e^{2i\xi_0} \cos^2 \theta_0 - \sin^2 \theta_0) &= 1 \\ e^{2i\alpha_0} (e^{-2i\xi_0} \cos^2 \theta_0 - \sin^2 \theta_0) &= 1. \end{aligned} \tag{20}$$

As for  $n = 1$ ,  $\zeta_0$  does enter this constraint; it is therefore an arbitrary function of  $t$  and  $x$ , which we denote simply by  $\zeta$  (see the discussion at the end of Section 4.1).

The first relation implies that  $\cos \xi_0 = 0$  (case 1) or  $\sin 2\theta_0 = 0$  (case 2). The first case corresponds to  $\xi_0 = (2k + 1)\pi/2$ ,  $k \in \mathbb{Z}$ . The second and third relations then transcribe into the single constraint  $\alpha_0 = (2k' + 1)\pi/2$ , with  $k' \in \mathbb{Z}$ . Note that  $\theta_0$  can then be an arbitrary function of  $t$  and  $x$ , as  $\zeta_0$ . This function will be simply denoted by  $\theta$ , just as  $\zeta$  denotes  $\zeta_0$ .

In contrast, the second case corresponds to  $\theta_0 = k\pi/2$ ,  $k \in \mathbb{Z}$ . If  $k = 2p + 1$ ,  $p \in \mathbb{Z}$  (case 2.1), the last two constraint relations deliver  $\alpha_0 = (2k' + 1)\pi/2$ , with  $k' \in \mathbb{Z}$ . The angle  $\xi_0$  is then arbitrary and will be denoted simply by  $\xi$ . If  $k = 2p$  (case 2.2), the last two constraint relations deliver  $\alpha_0 = k'\pi/2$ ,  $\xi_0 = \alpha_0 + k''\pi$ ,  $(k', k'') \in \mathbb{Z}^2$ .

Cases 1, 2.1 and 2.2 partly overlap. Indeed, jets obeying  $\theta_0 = k\pi$ ,  $\xi_0 = (2k + 1)\pi/2$  and  $\alpha_0 = (2k' + 1)\pi/2$  can be field under both case 1 and case 2. These are the only jets which can be field under both cases.

Let us now give the equations of motion of the continuous limit in cases 1, 2.1 and 2.2.

5.2. Equations of motion: case 1

$$\begin{aligned}
 & 2(\partial_T - (\cos^2 \theta)\partial_X)\psi^L - 2i(\bar{\alpha} + (\cos^2 \theta)\bar{\xi})\psi^L - e^{+i(\zeta - \xi_0)}(\sin 2\theta)\partial_X\psi^R \\
 & = (-\sin 2\theta)(\partial_X\theta) + i(\sin^2 \theta)(\partial_+\zeta)\psi^L \\
 & + e^{+i(\xi_0 + \zeta)}\left(i(\partial_-\zeta)\frac{\sin 2\theta}{2} - i\bar{\xi}(\sin 2\theta) + (\partial_T\theta) - (\partial_X\theta)(\cos 2\theta)\right)\psi^R
 \end{aligned} \tag{21}$$

and

$$\begin{aligned}
 & 2(\partial_T + (\cos^2 \theta)\partial_X)\psi^R - 2i(\bar{\alpha} - (\cos^2 \theta)\bar{\xi})\psi^R - e^{-i(\zeta - \xi_0)}(\sin 2\theta)\partial_X\psi^L \\
 & = (+\sin 2\theta)(\partial_X\theta) - i(\sin^2 \theta)(\partial_-\zeta)\psi^R \\
 & + e^{-i(\xi_0 + \zeta)}\left(i(\partial_+\zeta)\frac{\sin 2\theta}{2} - i\bar{\xi}(\sin 2\theta) - (\partial_T\theta) - (\partial_X\theta)(\cos 2\theta)\right)\psi^L.
 \end{aligned} \tag{22}$$

These equations can be put into the more compact form

$$\partial_T\Psi + (\cos \theta)P\partial_X\Psi = Q\Psi, \tag{23}$$

where  $\Psi = \psi^L b_L + \psi^R b_R$ ,

$$P = \begin{pmatrix} -\cos \theta & -e^{+i(\zeta - \xi_0)}\sin \theta \\ -e^{-i(\zeta - \xi_0)}\sin \theta & \cos \theta \end{pmatrix} \tag{24}$$

and

$$Q = \begin{pmatrix} Q_L^L & Q_R^L \\ Q_L^R & Q_R^R \end{pmatrix} \tag{25}$$

with

$$\begin{aligned}
 Q_L^L & = i(\bar{\alpha} + (\cos^2 \theta)\bar{\xi}) - \frac{\sin 2\theta}{2}(\partial_X\theta) + \frac{i}{2}(\sin^2 \theta)(\partial_+\zeta) \\
 Q_R^R & = i(\bar{\alpha} - (\cos^2 \theta)\bar{\xi}) + \frac{\sin 2\theta}{2}(\partial_X\theta) - \frac{i}{2}(\sin^2 \theta)(\partial_-\zeta) \\
 Q_L^R & = \frac{e^{+i(\xi_0 + \zeta)}}{2}\left(i(\partial_-\zeta)\frac{\sin 2\theta}{2} - i\bar{\xi}(\sin 2\theta) + (\partial_T\theta) - (\partial_X\theta)(\cos 2\theta)\right) \\
 Q_L^R & = \frac{e^{-i(\xi_0 + \zeta)}}{2}\left(i(\partial_+\zeta)\frac{\sin 2\theta}{2} - i\bar{\xi}(\sin 2\theta) - (\partial_T\theta) - (\partial_X\theta)(\cos 2\theta)\right).
 \end{aligned} \tag{26}$$

The operator  $P$  is self-adjoint and its eigenvalues are  $-1$  and  $+1$ . Two eigenvectors associated with these eigenvalues are

$$b_- = \left(\cos \frac{\theta}{2}\right)b_L + e^{i(-\zeta + \xi_0)}\left(\sin \frac{\theta}{2}\right)b_R, \tag{27}$$

$$b_+ = \left(\sin \frac{\theta}{2}\right)e^{i(\zeta + \xi_0)}b_L + \left(\cos \frac{\theta}{2}\right)b_R. \tag{28}$$

The family  $(b_-, b_+)$  forms an orthonormal basis of the two-dimensional spin Hilbert space, alternate to the original basis  $(b_L, b_R)$ . Let  $\Psi = \psi^- b_- + \psi^+ b_+$ . Eq. (23) transcribes into

$$\begin{aligned} \partial_T \psi^- - (\cos \theta) \partial_X \psi^- - i\bar{\alpha} \psi^- - i \cos \theta \bar{\xi} \psi^- + \frac{i}{2} ((\cos \theta - 1) \partial_+ \zeta) \psi^- + \frac{\partial_X \theta}{2} (\sin \theta) \psi^- &= 0 \\ \partial_T \psi^+ + (\cos \theta) \partial_X \psi^+ - i\bar{\alpha} \psi^+ + i \cos \theta \bar{\xi} \psi^+ - \frac{i}{2} ((\cos \theta - 1) \partial_- \zeta) \psi^+ - \frac{\partial_X \theta}{2} (\sin \theta) \psi^+ &= 0. \end{aligned} \quad (29)$$

Suppose now, to make the discussion definite, that  $\cos \theta$  is strictly positive and introduce in space–time  $\{(T, X)\}$  the Lorentzian, possibly curved metric  $G$  defined by its covariant components

$$(G_{\mu\nu}) = \begin{pmatrix} 1 & 0 \\ 0 & -\frac{1}{\cos^2 \theta} \end{pmatrix}, \quad (30)$$

where  $(\mu, \nu) \in \{T, X\}^2$ . This metric defines the canonical, scalar ‘volume’ element  $\mathcal{D}_G X = \sqrt{-G} dX = dX / \cos \theta$  in physical 1D  $X$ -space, where  $G$  is the determinant of the metric components  $G_{\mu\nu}$ . Dirac spinors are normalized to unity with respect to  $\mathcal{D}_G X$ , whereas  $\Psi$  is normalized to unity with respect to  $dX$ . We thus introduce  $\Phi = \Psi \sqrt{\cos \theta}$  and rewrite the equations of motion (29) in terms of  $\Phi$ . We obtain

$$\gamma^a \left[ e_a^\mu D_\mu \Phi + \frac{1}{2} \frac{1}{\sqrt{-G}} \partial_\mu (\sqrt{-G} e_a^\mu) \Phi \right] = 0, \quad (31)$$

where  $\mu \in \{T, X\}$ ,  $a \in \{0, 1\}$  and  $D_\mu = \partial_\mu - iA_\mu$  with

$$A_T = \bar{\alpha} + \frac{1 - \cos \theta}{2} \partial_X \zeta \quad (32)$$

and

$$A_X = -\bar{\xi} - \frac{1 - \cos \theta}{2 \cos \theta} \partial_T \zeta. \quad (33)$$

The usual 2D gamma matrices are

$$\gamma^0 = \begin{pmatrix} 0 & 1 \\ 1 & 0 \end{pmatrix}, \quad \gamma^1 = \begin{pmatrix} 0 & 1 \\ -1 & 0 \end{pmatrix}, \quad (34)$$

and the  $e_a^\mu$  are the components of the dyad (orthonormal basis)  $e_0 = e_T$  and  $e_1 = \cos \theta e_X$  on the original coordinate basis  $(e_T, e_X)$ . Eq. (31) is the standard [33] equation of motion for a massless Dirac spinor propagating in  $(1 + 1)$ -dimensional space–time under the combined influence of the gravitational field  $G$  and the electric field  $E$  deriving from  $A$ . Since the Dirac field is massless, its components are not coupled and evolve independently of each other. Each component follows a null geodesic of the gravitational field, and the electric field only modifies the energy along a given geodesic. Numerical simulations of a QW propagating radially in the gravitational field of a Schwarzschild black hole are presented in Section 6.3.

Let us conclude this section by commenting briefly on how the discrete gauge invariance presented in Section 2 transcribes in the present context. The continuous limit equation (18) is of course valid. Combining these with (32), (33) and keeping only the lowest order terms in  $\epsilon$  leads to the standard gauge transformation  $A'_0 = A_0 - \partial\phi/\partial T$  and  $A'_1 = A_1 - \partial\phi/\partial X$ . Just as it was the case in Section 4, the transformation law for  $\zeta$  does not contribute to the continuous gauge transformation, but it is not for the same reason. In Section 4, the potential  $A$  itself does not depend on  $\zeta$ . Here, the potential  $A$  does depend on  $\zeta$ , but the gauge transformation for  $\zeta$  generates terms of order  $\epsilon$  in the gauge transformation for  $A$ , and these terms vanish as  $\epsilon$  tends to zero. In the present context, the final, fourth equation in (18) reflects the fact that the gravitational field does not depend on the choice of gauge for the phase of the spinor  $\Psi$ .

### 5.3. Equations of motion: case 2.1

The equations of motion of the continuous limit read

$$\begin{aligned} 2\partial_T \psi^L - 2i\bar{\alpha} \psi^L &= +i(\partial_+ \zeta) \psi^L + 2\bar{\theta} e^{+i\zeta} (\cos \xi) \psi^R \\ 2\partial_T \psi^R - 2i\bar{\alpha} \psi^R &= -i(\partial_- \zeta) \psi^R - 2\bar{\theta} e^{-i\zeta} (\cos \xi) \psi^L, \end{aligned} \quad (35)$$

where  $\xi$  and  $\zeta$  are arbitrary functions of  $T$  and  $X$ . These equations are not PDEs, but *ordinary* differential equations (ODEs) in  $\psi^\pm$ . Thus, there is for example no propagation in this case. Technically, this comes from the fact that  $\theta_0$  is here constrained to be an uneven multiple of  $\pi/2$ .

#### 5.4. Equations of motion: case 2.2

The equations of motion read

$$\begin{aligned} 2\partial_- \psi^L - 2i(\bar{\alpha} + \bar{\xi}) \psi^L &= +2\bar{\theta} e^{i(2\alpha_0 + \zeta)} (\cos \xi_0) \psi^R \\ 2\partial_+ \psi^R - 2i(\bar{\alpha} - \bar{\xi}) \psi^R &= -2\bar{\theta} e^{i(2\alpha_0 - \zeta)} (\cos \xi_0) \psi^L, \end{aligned} \quad (36)$$

where  $\alpha_0$  is a multiple of  $\pi/2$ ,  $\xi_0 - \alpha_0$  is multiple of  $\pi$  and  $\zeta$  is an arbitrary function of  $T$  and  $X$ . Eq. (36) can be recast in the following compact form:

$$(i\gamma^0 D_0 + i\gamma^1 D_1 - \mathcal{M})\Psi = 0 \quad (37)$$

where  $D_\mu = \partial_\mu - iA_\mu$ ,  $\partial_0 = \partial_T$ ,  $\partial_1 = \partial_X$ ,  $A_0 = \bar{\alpha}$ ,  $A_1 = -\bar{\xi}$ ,  $\mathcal{M} = \text{diag}(m^-, m^+)$  and  $m^\mp = \pm i\bar{\theta} \exp\{i(2\alpha_0 \pm \zeta)\} (\cos \xi_0)$ . This equation describes the propagation in flat space-time of a Dirac spinor  $\Psi$  coupled to the potential  $A$  and with a mass tensor  $\mathcal{M}$ .

## 6. Numerical simulations

### 6.1. Basics

In order to ascertain the validity of the continuous limits that were derived above, we wish to compare numerical solutions of the QW defined by the finite difference Eqs. (1) and (2) with the corresponding Dirac-type PDEs defined by Eqs. (31) and (17).

While the numerical integration of the QW finite difference equations poses no particular problem, controlling the error on numerical solutions of PDEs is a more involved matter. This hurdle can be avoided in the special case where the mass terms cancels, because one can then compare the numerical solutions of the QW finite difference equations with the numerical solutions of the ODEs defining the *characteristics* of the massless Dirac PDE (see Section 6.3).

We have chosen to use Fourier pseudo-spectral methods [34], for their precision and ease of implementation. We therefore restrict ourselves to  $2\pi$ -periodic boundary conditions. A generic field  $\psi(x)$  is thus evaluated on the  $n$  collocation points  $x_j = 2\pi j/n$ , with  $j = 0, n-1$  as  $\psi_j = \psi(x_j)$ . The discrete Fourier transforms are standardly defined as

$$\begin{aligned} \psi(x_j) &= \sum_{k=-n/2}^{n/2-1} \exp(ikx_j) \hat{\psi}_k \\ \hat{\psi}_k &= \frac{1}{n} \sum_{j=0}^{n-1} \psi(x_j) \exp(-ikx_j). \end{aligned} \quad (38)$$

These sums can be evaluated in only  $n \log(n)$  operations by using Fast Fourier Transforms (FFTs). Spatial derivatives of fields are evaluated in spectral space by multiplying by  $ik$  and products are evaluated in physical space.

The original QW Eqs. (1) and (2) can also be simply cast in this setting, as the translation operator  $\psi_j \rightarrow \psi_{j\pm 1}$  is represented in Fourier space by  $\hat{\psi}_k \rightarrow \hat{\psi}_k \exp(\pm i k 2\pi/n)$ . In this setting, the continuous limit is automatically taken when  $n$  is increased.

### 6.2. QWs in constant a uniform electric field

As explained in Section 2, the QWs and the Dirac equation exhibit a  $U(1)$  gauge invariance. All choices of gauge thus correspond to the same physics. Within a pseudo-spectral code, the right gauge to work with a 1D constant uniform electric field  $E$  is  $A_0 = 0$ ,  $A_1 = -E T$ ; in particular, the other ‘natural choice’  $A_0 = -E X$ ,  $A_1$  breaks the spatial periodicity condition. In all QW simulations, the retained choice of gauge has been implemented by choosing the following numerical values:

$$\begin{aligned} \alpha(T, X) &= 0 \\ \xi(T, X) &= 1.1 T \\ \zeta(T, X) &= \frac{\pi}{2} \\ \theta(T, X) &= 0.24. \end{aligned}$$

We used initial data consisting of Gaussian wave packets of positive energy solutions to the free Dirac equation. The Gaussian widths  $\sigma_x$  are such that they are well resolved within the used resolutions so that spectral convergence is ensured.

As discussed above (see end of Section 6.1) the QW and its Dirac continuous limit can be jointly simulated within the same pseudo-spectral algorithm. This allows for a very simple, direct evaluation of the discrepancy between the QW and the corresponding solution of the Dirac equation. This discrepancy can be measured by the relative difference  $\delta N_{\text{rel}}$  between the density of the QW and the density of the solution of the Dirac equation.

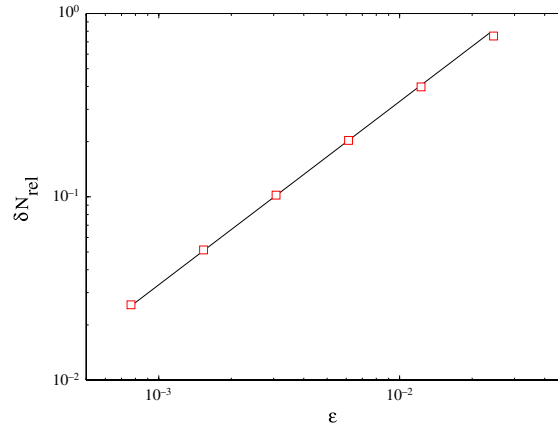


**Fig. 1.** Relative difference between the density of the QW and the density of the solution of the Dirac equation  $\delta N_{\text{rel}} = \sqrt{\langle (N_{\text{QW}} - N_D)^2 \rangle} / \langle N_D \rangle$  plotted at  $T = 100$  versus  $\epsilon = \Delta X$  in Log–Log representation. We have plotted the relative difference in the same conditions as in Fig. 2(a) but for five different resolutions (i.e. value of  $\epsilon$ ): from the left  $n = 2^8, 2^9, 2^{10}, 2^{11}, 2^{12}, 2^{13}$ . The solid black line represents the expected  $\epsilon^1$  scaling.

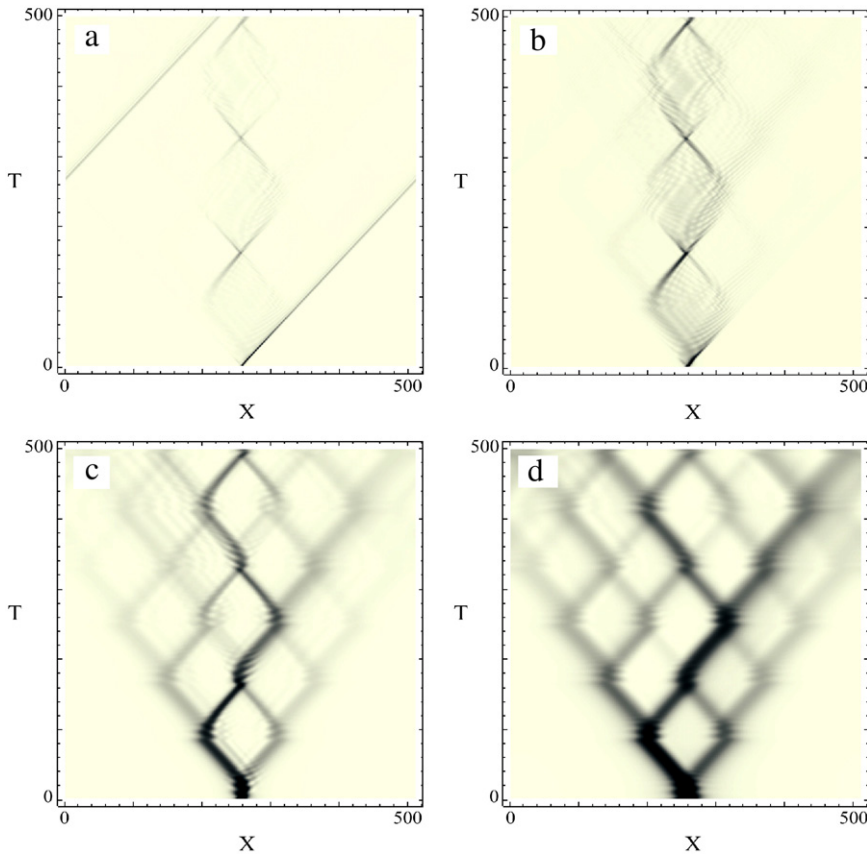


**Fig. 2.** Quantum simulation of Eqs. (1) and (2) representing a Dirac particle in a constant and static electric background (see Section 4.2 and Eq. (39)). The initial condition is a Gaussian wave packet of positive energy solutions with width  $\sigma_X = 0.005$  in (a), 0.01 in (b), 0.03 in (c), 0.08 in (d) and resolution  $n = 2^9$ .

Fig. 1 shows that such a typical relative difference scales as  $\epsilon$ , as expected. Indeed, for a single time-step, the discrepancy is theoretically of order  $\epsilon^2$ . Thus, after a fixed time  $T = O(\epsilon^{-1})$ , the discrepancy is of order  $\epsilon^{-1}\epsilon^2 = \epsilon$ .

This result confirms that QWs can be used to simulate Dirac dynamics in constant electric field, as was done for example in Refs. [35,36]. Both QW and Dirac dynamics are very rich, as exemplified by Fig. 2, which compare with Fig. 2 of Ref. [35] and Fig. 3 of Ref. [36].

Note that, as  $\sigma_x$  increases, the spatial dispersion of the wave packet also increases which makes the time evolution of the density more complex. The solution which is initially a positive energy planar wave starts to oscillate between positive and negative modes under the action of the constant electric field displaying high-frequency Zitterbewegung in Fig. 2(c)–(d). Offering new results of the Dirac dynamics in the presence of an electric field is not the purpose of this article. Let us conclude this section by offering instead a brief historical overview of the very large literature already existing on the topic.

In 1929, Klein studied a relativistic scalar particle moving in an external step function potential. He found a paradox that, in the case of a strong potential, the reflected flux is larger than the incident flux although the total flux is conserved [37]. Sauter studied this problem for a Dirac spin 1/2 particle by considering a potential corresponding to a electric field with constant value  $E_0$  on a given interval. He found an expression for the transmission coefficient of the wave through the electric potential barrier from the negative energy state to positive energy states [38]. This remarkable phenomenon was related, in 1936, to positron–electron pair creations by Heisenberg and his student Hans Euler [39].

Of course, in order to deal with anti-particles a massive reinterpretation of the Dirac equation theory is necessary [40], leading to modern field theory and quantum electrodynamics. The modern formula for pair creation in a constant external electric field was delivered, in 1951, by Schwinger [41]. It involves the same dominant exponential term  $\exp(-\pi \frac{m_e^2 c^3}{\hbar e E})$  that was derived, 20 years before, by Sauter. A detailed review of these historical developments is given in the first sections of Ref. [42].

### 6.3. QWs in Schwarzschild black hole

A Schwarzschild black hole is a spherically symmetric solution of the Einstein equation in vacuo. The corresponding 4D metric reads, in dimensionless Lemaître coordinates  $(\tau, \rho, \theta, \phi)$  [43]:

$$ds^2 = d\tau^2 - \frac{r_g}{r} d\rho^2 - r^2 d\Omega, \tag{39}$$

where  $r(\tau, \rho) = r_g^{1/3} [\frac{3}{2}(\rho - \tau)]^{2/3}$ ,  $d\Omega = d\theta^2 + (\sin^2 \theta) d\phi^2$ . The event horizon is located at  $r = r_g$ , that is,  $\rho = \tau + (2/3)r_g$ , and the singularity is located at  $r = 0$  i.e.  $\rho = \tau$ . The exterior of the black hole is the domain  $r > r_g$ . The range of variations for the Lemaître coordinates is  $\tau \geq 0, \rho \geq \tau$ , that is,  $r(\tau, \rho) \geq 0, 0 \leq \theta \leq \pi, 0 \leq \phi < 2\pi$ .

Because of the spherical symmetry, a point mass which starts its motion radially will go on moving radially. Radial motion can be studied by introducing the 2D metric  $g$ , also singular at  $r = 0$ , with covariant components  $g_{\tau\tau} = 1, g_{\rho\rho} = -r_g/r, g_{\tau\rho} = g_{\rho\tau} = 0$ . The null geodesics of  $g$  are defined by  $d\tau = \pm (r_g/r(\tau, \rho))^{1/2} d\rho$ . Note that the 2D projection of the horizon on the  $(\tau, \rho)$ -plane coincides with a null geodesics of  $g$ .

We now identify the dimensionless time  $T$  with the time coordinate  $\tau$  and the dimensionless space variable  $X$  with  $\lambda\rho$ , where  $\lambda$  is an arbitrary strictly positive real number (see Fig. 3). The ‘radius’  $r$  can then be expressed as a function of  $T$  and  $X$ :

$$r(T, X) = \left[ \frac{3}{2} \left( \frac{X}{\lambda} - T \right) \right]^{2/3} r_g^{1/3}, \tag{40}$$

and the components of  $g$  in the coordinate basis associated to  $T$  and  $X$  are  $g_{TT} = 1, g_{XX} = -r_g/(\lambda^2 r), g_{TX} = g_{XT} = 0$ . Note that the condition  $\rho \geq \tau$  transcribes into  $X \geq \lambda T$ .

Let  $\mathcal{D}$  be the domain where  $-g_{XX} \geq 1$ . This domain is characterized, in  $(T, X)$  coordinates, by the condition

$$X \leq \lambda T + \frac{2}{3\lambda^2} r_g. \tag{41}$$

In  $\mathcal{D}$  the metric  $g$  can be identified with the metric  $G$  (see Eq. (30)). This identification defines an angle  $\theta$  which depends on  $T$  and  $X$  by

$$(\cos \theta)(T, X) = \lambda \sqrt{\frac{r(T, X)}{r_g}}. \tag{42}$$

A QW in  $\mathcal{D}$  can be defined by complementing this choice of  $\theta$  by a choice of the other three angles. All simulations were done with

$$\begin{aligned} \alpha(T, X) &= 0 \\ \xi(T, X) &= \pi \\ \zeta(T, X) &= \frac{\pi}{2}. \end{aligned} \tag{43}$$

This QW has already been considered in Ref. [32].

The condition defining  $\mathcal{D}$  can be rewritten as  $r \leq r_g/\lambda^2$ . The domain  $\mathcal{D}$  thus includes, for all  $\lambda$ , the singularity located at  $r = 0$ . For  $\lambda > 1, r_g/\lambda^2 < r_g$  and  $\mathcal{D}$  is then entirely located inside the horizon. For  $\lambda = 1, \mathcal{D}$  coincides with the interior of the horizon, and  $\mathcal{D}$  extends outside the horizon for  $\lambda < 1$ .

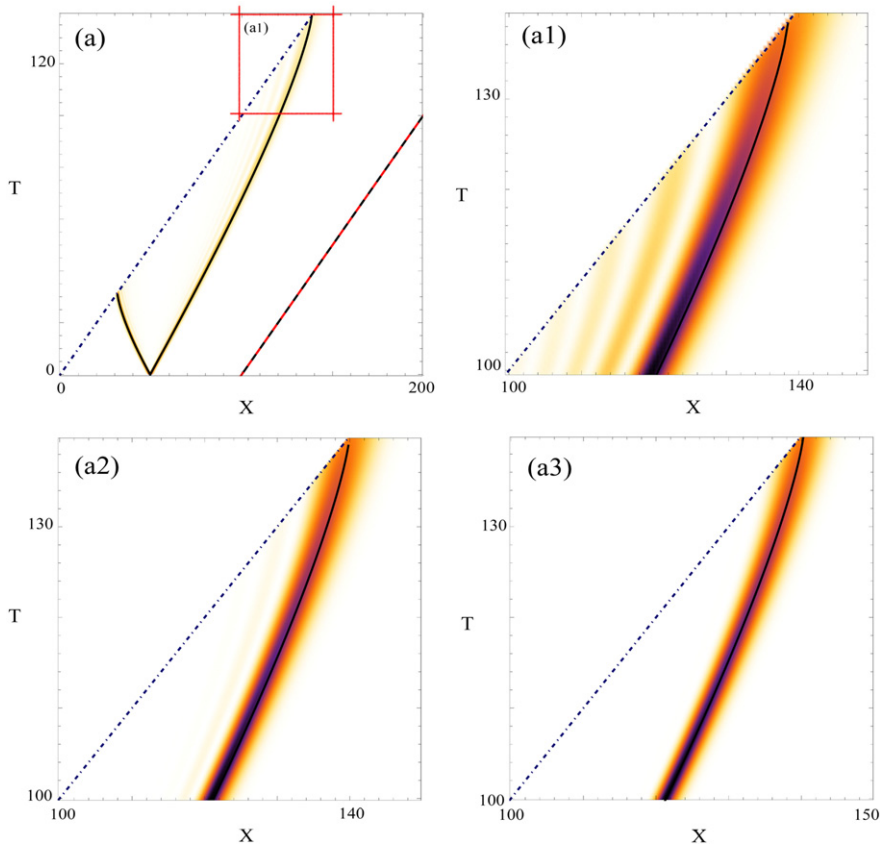


**Fig. 3.** (Color online) Time evolution density of the QW vs. null geodesics (solid curves) of the 2D Schwarzschild metric with  $\lambda = 1$ . The initial condition is  $\Psi(0, X) = \sqrt{N_0(X)}(b_L + Ib_R)$  with an initial Gaussian density  $N_0$  of  $\sigma_X = 0.5$  centered on  $X_0 = 50.5$ . The singularity is represented by the dotted and dashed line on the left and the horizon (which is a null geodesic) is represented by the dashed line. The two branches of the QW which starts inside the horizon end up on the singularity. The (red) solid line represents the limit of the definition domain  $\mathcal{D}$  of the QW. In (a1) note that the right branch of the QW lags slightly behind the null geodesic when approaching the  $r = 0$  singularity. The agreement between the geodesics and the density profile of the walk gets better as we increase the resolution of the simulation: 200 gridpoints in (a1), 800 in (a2) and 1600 in (a3).

Ref. [32] offers plots of the spatial density  $|\Psi(T, X)|^2$  for several initial conditions. These plots confirm that the QW follows to a great accuracy the radial null geodesics of the Schwarzschild metric, except perhaps as the QW approaches the singularity. This phenomenon is explored in detail by Fig. 3. The plots reveal the existence of interesting ‘interferences’ near the singularity (see (a1) and (a2)), which seem to disappear as  $\epsilon$  tends to zero.

## 7. Conclusion

We have revisited the continuous limit of discrete time QWs on the line, keeping every step or only one step out of two. We have identified all families of walks which admit a continuous limit and obtained the associated PDEs. In all cases but one, the PDE describes the propagation of a Dirac fermion coupled to an electric field and, possibly, to a general relativistic gravitational field. We have also illustrated these conclusions by new numerical simulations.

Let us now briefly discuss the above results.

As mentioned in the introduction, all above literal computations are based on a new method first introduced in Refs. [30–32,29]. New to this article is all the material presented in Section 5. The Dirac equation obtained in Section 4 has already been presented in Refs. [30–32,29], but without the important discussion of the  $U(1)$  gauge invariance. The discrete gauge invariance presented in Section 2 is also new. Let us mention in this context that QWs coupled to a uniform and constant electric field have also been considered theoretically and experimentally in Refs. [44,45]. These so-called ‘electric walks’ are particular cases of the walks considered in Refs. [30–32,29] and in Section 4 of the present article. In Ref. [44], the constant and uniform electric field is put by hand on the equations of motion of the walks. In contrast, the approach developed in the present article makes it clear that the electric field is simply a manifestation of the time- and space-dependence of the angles defining the walks. This approach also allows for a straightforward generalization to nonconstant and/or nonuniform electric fields (Sections 4 and 5), and to gravitational fields 5. The electric and gravitational fields coupled to the QWs thus clearly appear as synthetic gauge fields [46].

Experiments with time- and space-dependent coins are now possible thanks to at least two recently developed techniques [47,48]. For example, one can use integrated waveguide circuits [47] where the quantum coin and step operator at a given point and time corresponds to a precise beamsplitter that can be individually set. These techniques could be used to implement experiments where arbitrary electric and/or gravitational fields are simulated by properly choosing the time- and space-dependence of the angles  $\alpha$ ,  $\xi$  and  $\theta$ .

The work presented in this article should be extended in several directions. One should first determine how the new method works, and what it delivers, when one keeps only one step out of  $n$  for arbitrary  $n > 2$ . Extensions to higher dimensional space and/or to higher dimensional Hilbert space are also desirable. In particular, the fact that some QWs on the line can be interpreted as the propagation of charged massless Dirac fermions suggests that QWs could be useful in modeling charge transport in graphene [49,50], both natural and artificial [51,52]. Let us note that the inherent discreteness would give QWs a strong computational advantage over the more traditional models based on PDEs. Finally, determining systematically the continuous limit of nonlinear QWs [53] and of walks in random media [54] should also prove interesting.

## References

- [1] R.P. Feynman, A.R. Hibbs, Quantum Mechanics and Path Integrals, in: International Series in Pure and Applied Physics, McGraw-Hill Book Company, 1965.
- [2] Y. Aharonov, L. Davidovich, N. Zagury, Quantum random walks, Phys. Rev. A 48 (1993) 1687.
- [3] D.A. Meyer, From quantum cellular automata to quantum lattice gases, J. Stat. Phys. 85 (1996).
- [4] E. Farhi, S. Gutmann, Quantum computation and decision trees, Phys. Rev. A 58 (1998) 915.
- [5] H. Schmitz, R. Matjeschek, Ch. Schneider, J. Glueckert, M. Enderlein, T. Huber, T. Schaez, Quantum walk of a trapped ion in phase space, Phys. Rev. Lett. 103 (9) (2009) 090504.
- [6] F. Zähringer, G. Kirchmair, R. Gerritsma, E. Solano, R. Blatt, C.F. Roos, Realization of a quantum walk with one and two trapped ions, Phys. Rev. Lett. 104 (2010) 100503.
- [7] A. Schreiber, K.N. Cassemiro, A. Gábris, V. Potoček, P.J. Mosley, E. Andersson, I. Jex, Ch. Silberhorn, Photons walking the line, Phys. Rev. Lett. 104 (5) (2010) 050502.
- [8] Michal Karski, Leonid Förster, Jai-Min Cho, Andreas Steffen, Wolfgang Alt, Dieter Meschede, Artur Widera, Quantum walk in position space with single optically trapped atoms, Science 325 (5937) (2009) 174–177.
- [9] Alberto Peruzzo, Mirko Lobino, Jonathan C.F. Matthews, Nobuyuki Matsuda, Alberto Politi, Konstantinos Poullos, Xiao-Qi Zhou, Yoav Lahini, Nur Ismail, Kerstin Wörhoff, Yaron Bromberg, Yaron Silberberg, Mark G. Thompson, Jeremy L. O'Brien, Quantum walks of correlated photons, Science 329 (5998) (2010) 1500–1503.
- [10] L. Sansoni, F. Sciarrino, G. Vallone, P. Mataloni, A. Crespi, R. Ramponi, R. Osellame, Two-particle bosonic-fermionic quantum walk via 3D integrated photonics, Phys. Rev. Lett. 108 (1) (2012) 010502.
- [11] B.C. Sanders, S.D. Bartlett, B. Tregenna, P.L. Knight, Two-particle bosonic-fermionic quantum walk via 3D integrated photonics, Phys. Rev. A 67 (2003) 042305.
- [12] B. Perets, Y. Lahini, F. Pozzi, M. Sorel, R. Morandotti, Y. Silberberg, Realization of quantum walks with negligible decoherence in waveguide lattices, Phys. Rev. Lett. 100 (2008) 170506.
- [13] D. Giulini, E. Joos, C. Kiefer, J. Kupsch, I.-O. Stamatescu, H.D. Zeh, Decoherence and the Appearance of a Classical World in Quantum Theory, Springer-Verlag, Berlin, 1996.
- [14] A. Ambainis, Quantum walk algorithm for element distinctness, SIAM J. Comput. 37 (2007) 210–239.
- [15] F. Magniez, J. Roland, A. Nayak, M. Santha, Search via quantum walk, in: SIAM Journal on Computing—Proceedings of the Thirty-Ninth Annual ACM Symposium on Theory of Computing, ACM, New York, 2007.
- [16] C. Aslangul, Quantum dynamics of a particle with a spin-dependent velocity, J. Phys. A 38 (2005) 1–16.
- [17] S. Bose, Quantum communication through an unmodulated spin chain, Phys. Rev. Lett. 91 (2003) 207901.
- [18] D. Burgarth, Quantum state transfer with spin chains, University College London, Ph.D. Thesis, 2006.
- [19] S. Bose, Quantum communication through spin chain dynamics: an introductory overview, Contemp. Phys. 48 (1) (2007) 13–30.
- [20] E. Collini, C.Y. Wong, K.E. Wilk, P.M.G. Curmi, P. Brumer, G.D. Scholes, Coherently wired light-harvesting in photosynthetic marine algae at ambient temperature, Nature 463 (2010) 644.
- [21] G.S. Engel, T.R. Calhoun, R.L. Read, T.-K. Ahn, T. Manal, Y.-C. Cheng, R.E. Blankenship, G.R. Fleming, Evidence for wavelike energy transfer through quantum coherence in photosynthetic systems, Nature 446 (2007) 782.
- [22] A.J. Bracken, D. Ellinas, I. Smykalis, Free-dirac-particle evolution as a quantum random walk, Phys. Rev. A 75 (2007) 022322.
- [23] Ph. Blanchard, M.-O. Hongler, Quantum random walks and piecewise deterministic evolutions, Phys. Rev. Lett. 92 (2004) 120601–1–120601–4.
- [24] C.M. Chandrasekhar, S. Banerjee, R. Srikanth, Relationship between quantum walks and relativistic quantum mechanics, Phys. Rev. A 81 (2010) 062340.
- [25] P.L. Knight, E. Roldàn, J.E. Sipe, Quantum walk on the line as an interference phenomenon, Phys. Rev. A 68 (2003) 020301.
- [26] F.W. Strauch, Relativistic quantum walks, Phys. Rev. A 73 (2006) 054302.
- [27] F.W. Strauch, Relativistic effects and rigorous limits for discrete-time and continuous-time quantum walks, J. Math. Phys. 48 (2007) 082102.
- [28] F.W. Strauch, Connecting the discrete- and continuous-time quantum walks, Phys. Rev. A 74 (2006) 030301.
- [29] F. Debbasch, G. Di Molfetta, D. Espaze, V. Foulonnet, Propagation in quantum walks and relativistic diffusions, Phys. Scr. 151 (2012) 014044.
- [30] G. Di Molfetta, F. Debbasch, Discrete-time quantum walks: continuous limit and symmetries, J. Math. Phys. 53 (2012) 123302.
- [31] G. Di Molfetta, F. Debbasch, Discrete-time quantum walks: continuous limit in  $1 + 1$  and  $1 + 2$  dimension, J. Comput. Theor. Nanosci. 10 (7) (2012) 1621–1625.
- [32] G. Di Molfetta, F. Debbasch, M. Brachet, Quantum walks as massless dirac fermions in curved space, Phys. Rev. A 88 (2013).
- [33] A. Sinha, R. Roychoudhury, Dirac equation in  $(1 + 1)$ -dimensional curved space-time, Int. J. Theor. Phys. 33 (1994) 1511–1522.
- [34] D. Gottlieb, S.A. Orszag, Numerical Analysis of Spectral Methods, SIAM, Philadelphia, 1977.
- [35] D. Witthaut, Quantum walks and quantum simulations with Bloch-oscillating spinor atoms, Phys. Rev. A 82 (2010) 033602.
- [36] S. Longhi, Bloch-zener quantum walk, J. Phys. B: At. Mol. Opt. Phys. 45 (2010) 225504.
- [37] O. Klein, Die reflexion von elektronen an einem potenzialsprung nach der relativistischen dynamik von Dirac, Z. Phys. 53 (3–4) (1929) 157–165.
- [38] Fritz Sauter, Über das verhalten eines elektrons im homogenen elektrischen feld nach der relativistischen theorie Diracs, Z. Phys. 69 (11–12) (1931) 742–764.
- [39] W. Heisenberg, H. Euler, Folgerungen aus der diracschen theorie des positrons, Z. Phys. 98 (11–12) (1936) 714–732.
- [40] J.D. Bjorken, S.D. Drell, Relativistic Quantum Mechanics, in: International Series in Pure and Applied Physics, McGraw-Hill, 1964.
- [41] Julian Schwinger, On gauge invariance and vacuum polarization, Phys. Rev. 82 (1951) 664–679.
- [42] Remo Ruffini, Gregory Vereshchagin, She-Sheng Xue, Electron-positron pairs in physics and astrophysics: from heavy nuclei to black holes, Phys. Rep. 487 (1–4) (2010) 1–140.
- [43] G. Lemaître, L'univers en expansion, Ann. Soc. Sci. Brux. A 53 (1933) 51–85.

- [44] M. Genske, W. Alt, A. Steffen, A.H. Werner, R.F. Werner, D. Meschede, A. Alberti, Electric quantum walks with individual atoms, *Phys. Rev. Lett.* 110 (2013) 190601.
- [45] C. Cedzich, T. Rybár, A.H. Werner, A. Alberti, M. Genske, R.F. Werner, Propagation of quantum walks in electric fields, *Phys. Rev. Lett.* 111 (2013) 160601.
- [46] J. Dalibard, F. Gerbier, G. Juzeliūnas, P. Öhberg, Artificial gauge potential for neutral atoms, *Rev. Modern Phys.* 83 (2010) 1523.
- [47] A. Crespi, R. Osellame, R. Ramponi, V. Giovannetti, R. Fazio, L. Sansoni, F. De Nicola, F. Sciarrino, P. Mataloni, Anderson localization of entangled photons in an integrated quantum walk, *Nat. Photonics* 7 (2013) 322–328.
- [48] A. Schreiber, A. Gábris, P.P. Rohde, K. Laiho, M. Štefaňák, V. Potoček, C. Hamilton, I. Jex, C. Silberhorn, A 2D quantum walk simulation of two-particle dynamics, *Science* 336 (2012) 55.
- [49] K.S. Novoselov, A.K. Geim, S.V. Morozov, D. Jiang, M.I. Katsnelson, I.V. Grigorieva, S.V. Dubonos, A.A. Firsov, Two-dimensional gas of massless dirac fermions in graphene, *Nature* 438 (2005) 197–200.
- [50] D.C. Elias, R.V. Gorbachev, A.S. Mayorov, S.V. Morozov, A.A. Zhukov, P. Blake, L.A. Ponomarenko, I.V. Grigorieva, K.S. Novoselov, F. Guinea, A.K. Geim, Dirac cones reshaped by interaction effects in suspended graphene, *Nature* 7 (2011) 701–704.
- [51] M. Polini, F. Guinea, M. Lewenstein, H.C. Manoharan, V. Pellegrini, Artificial honeycomb lattices for electrons, atoms and photons, *Nat. Nanotechnol.* 8 (2013) 625–633.
- [52] T. Uehlinger, G. Jotzu, M. Messer, D. Greif, W. Hofstetter, U. Bissbort, T. Esslinger, Artificial graphene with tunable interactions, *Phys. Rev. Lett.* 111 (2013) 185307.
- [53] C. Navarrete-Benlloch, A. Perez, Eugenio Roldan, Nonlinear optical galton board, *Phys. Rev. A* 75 (2010) 062333.
- [54] C.M. Chandrashekar, Th. Busch, Quantum percolation and anderson transition point for transport of a two-state particle, 2013. ArXiv Preprint arXiv:1303.7013.